

AD 68 03956

MECHANISMS OF LASER-SURFACE INTERACTIONS

By

J. F. Ready
E. Bernal G.

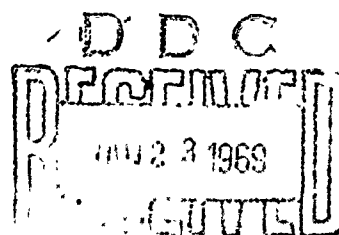
SEMI-ANNUAL REPORT

To

Ballistic Research Laboratories
Aberdeen Proving Ground, Maryland

Contract No. DA-18-001-AMC-1040(X) Modification No. 2

November 1968



Presented by
Honeywell Inc.

CORPORATE RESEARCH CENTER
Hopkins, Minnesota

Reproduced by the
CLEARINGHOUSE
for Federal Scientific & Technical
Information Springfield Va. 22151

This document has been approved for public release
and sale; its distribution is unlimited.

48

DISCLAIMER NOTICE

**THIS DOCUMENT IS BEST QUALITY
PRACTICABLE. THE COPY FURNISHED
TO DTIC CONTAINED A SIGNIFICANT
NUMBER OF PAGES WHICH DO NOT
REPRODUCE LEGIBLY.**

MECHANISMS OF LASER-SURFACE INTERACTIONS

By

J. F. Ready

E. Bernal G.

SEMI-ANNUAL REPORT

To

Ballistic Research Laboratories

Aberdeen Proving Ground, Maryland

Contract No. DA-18-001-AMC-1040(X) Modification No. 2

November 1968

"Delivered by Honeywell Inc., Research Center, pursuant to Contract No. DA-18-001-AMC-1040(X). Government's use controlled by the provisions of Articles 51 and 26 of Title 11 of the contract which are ASPR 9-107.2 and 9-203.1 and 9-203.4, respectively."

Presented by

Honeywell Inc.

CORPORATE RESEARCH CENTER

Hopkins, Minnesota

This document has been approved for public release and sale; its distribution is unlimited.

ABSTRACT

This report describes investigations of the mechanisms by which high power laser radiation interacts with absorbing surfaces. Construction of a carbon dioxide laser used in this work is described, along with preliminary spectroscopic observations of the emission produced when this laser radiation interacts with a glass target. Measurements of ion emission produced by a ruby laser beam with flux densities of the order of 1000 megawatts per square centimeter incident on a tungsten target have been analyzed. From the results it is estimated that particle densities of the order of 10^{20} per cubic centimeter are produced near the target surface. A computer program using these particle densities has been employed to calculate the expected amount of heating produced by absorption of the incident laser radiation in a sodium plasma of this density. The results indicate that rapid heating to temperatures of the order of tens of eV is possible within the time of the laser pulse duration.

TABLE OF CONTENTS

<u>Section</u>		<u>Page</u>
I.	INTRODUCTION	1
II.	CARBON DIOXIDE LASER WORK	4
	A. Laser Construction	4
	B. Q-Switching of CO ₂ Laser	6
	C. Spectroscopy of Laser-Produced Plasma	6
	D. Spectroscopic Measurements	7
III.	WORK ON RUBY LASER AND HEMISPHERICAL INTERACTION CHAMBER	16
	A. Picosecond Pulses	16
	B. Ruby Laser Measurements	20
IV.	ANALYSIS	25
	A. Calculated Plasma Heating	25
	B. Expansion of Heated Plasma	29
	C. Comparison to Experiment	30
	D. Effect of Surface on Plasma Isotropy	33
V.	CONCLUSIONS	37
	REFERENCES	40

LIST OF ILLUSTRATIONS

<u>Figure</u>		<u>Page</u>
II-1.	Schematic of CO ₂ Laser.	5
II-2.	Experimental Arrangement for Spectroscopic Measurements.	9
II-3.	Plasma Produced with Glass Target.	10
II-4.	Spectrum of Plasma Produced by Irradiation of Glass.	11
III-1.	Experimental Arrangement for Two-Photon Fluorescence.	17
III-2.	Nanosecond Duration Structure in Laser Pulses.	19
III-3.	Output of Disc Collectors for High Laser Power.	21
III-4.	Output of Bipolar Collector for High Laser Power.	23
IV-1.	Calculated Heating of Sodium Plasma with no Expansion.	28
IV-2.	Calculated Heating of Sodium Plasma with Expansion.	31

I. INTRODUCTION

This report describes investigations of particle emission produced in laser-surface interactions and discusses work which continues along lines described in previous reports.⁽¹⁻⁷⁾ In order to understand the present report, we present here a brief summary of previous results. The methods and aims of the investigations described in the present report depend on the earlier results and some knowledge of this background is necessary.

A time-of-flight spectrometer has been used to measure ion emission produced by interaction of ruby laser radiation with flux densities of the order of 50 megawatts/cm² with metallic targets. The ions were found to be mainly alkali metals with energies of the order of several hundred electron volts. Total ion production of the order of 10⁹ ions per laser pulse was indicated. Neutral molecule emission was studied using a quadrupole mass spectrometer under similar conditions of laser bombardment and was found to consist of thermally desorbed gases such as hydrogen, carbon monoxide, and carbon dioxide. Pulses of high energy neutral molecules with energies of the order of 100 eV were produced along with the thermally desorbed gases.

Additional studies were performed in a hemispherical interaction chamber with shielded disc collectors around the periphery of the hemisphere and the laser-illuminated target at the center. This geometry was used to perform measurements of the angular distribution of the particle emission. In addition to the disc collectors, we employed a bipolar collector which we feel to be a better method of indicating the total ion production. This collector indicated a total ion production of the order of 10¹³ ions per laser pulse, much higher than was found in the time-of-flight spectrometer. These results indicate that the bulk of the material travels as a neutral plasma. In addition to direct collection of positive ions, secondary electron emission produced at the collector surfaces is important.

The measurements in this present report depend on these earlier results and extend them in some cases. The ruby laser measurements in the hemispherical interaction chamber have been extended to laser flux densities of the order of 1000 megawatts/cm². The currents observed both from the bipolar collector and from the ordinary collectors increase about one order of magnitude, but qualitatively have the same general features as were observed at lower flux densities. We shall discuss the question of why the qualitative effects are similar in Section IV. The results are also analyzed to indicate that ion densities of the order of 10²⁰ per cubic centimeter near the target surface may occur during the time of the laser pulse.

Using this value for particle density, we have extended calculations on a computer program used previously⁽⁶⁾ to investigate the heating of a plasma exposed to a laser beam. When lower ion densities, as indicated by the time-of-flight spectrometer results, were used as input for this program, the results indicated that little heating would be produced. At the higher densities, we find that heating can occur very rapidly. Heating to temperatures of tens of electron volts in a time comparable to the duration of the laser pulse may be expected under our experimental conditions. In a previous report⁽⁵⁾ we had already discussed the pulse shapes expected when a gas heated to a temperature of the order of 10 or 20 electron volts is allowed to expand in an adiabatic free expansion. We had concluded that the pulse shapes observed in the time-of-flight spectrometer and in the hemispherical interaction chamber could be explained on this basis.

In addition we describe a search for the presence of picosecond duration substructure in the laser pulse. If such substructure is present, it would influence our experimental results because the instantaneous power would be much higher. Early preliminary measurements using a two-photon fluorescence technique in a dye solution indicated an essentially negative result. While picosecond pulses may have been occasionally present, they were usually absent. However, since the time of this experiment, operating conditions in the laser changed and a considerable amount of nanosecond duration structure on the laser pulse has developed which indicates an enhanced degree of mode-

locking. Therfore, the search for picosecond duration substructure should be renewed under the present operating conditions.

We have also continued our efforts to employ CO₂ lasers for investigation of the laser-surface interaction. During this report period a CO₂ laser with a continuous output of the order of 55 watts has been constructed. Spectroscopic observations of the plasmas produced when this radiation is incident on a glass target have been initiated. Lines of the alkali metals have been observed and identified. In the next period we intend to begin Q-switching this laser.

The details of the work on the CO₂ laser and its use form Section II. Section III describes the work performed using the ruby laser and the hemispherical interaction chamber. In Section IV the analysis and computer results are presented.

II. CARBON DIOXIDE LASER WORK

A. LASER CONSTRUCTION

A carbon dioxide laser with a 1.25 meter discharge length was constructed. It is shown in Figure II-1. It consists of a water-cooled pyrex tube with one electrode on each end and rotatable joints at the ends of the tube. The use of rotatable joints allows one to use either Brewster angle windows or mirrors that are internal to the cavity. We have used Brewster windows made of Irtran 2 as well as sodium choloride. In the early tests of the laser the Irtran windows were used because of the undesirable hygroscopic and other thermal properties of sodium chloride. However, we have now eliminated those windows in favor of rock salt because the scattering loss is extremely large over the optical path required for Brewster windows. In fact, with all other parameters held constant, the output of the laser dropped from 55 watts at a discharge voltage of 16 kilovolts and a current of 35 milliamperes using sodium choloride Brewster windows to 15 watts using Irtran windows.

The cavity for the laser consists of a totally reflecting gold-coated mirror with a three meter radius of curvature and a flat Irtran 2 output mirror with an 85% reflecting coating on one side and an antireflecting coating on the other side. The lowest order mode in this configuration fills the 20 millimeter aperture of the laser tube quite adequately and the output is almost always in the TEM_{00} mode. We have not investigated the wavelength characteristics of the output since these have not been of interest so far.

In our use of the 125 centimeter CO_2 laser the power output has been limited by the 35 milliampere limitation of our power supply. It appears that in the future we will wish to increase the output of the laser by extending the capability of the power supply. Judging from the published literature, ⁽⁸⁾ it should be possible to obtain 80 to 100 watts of output from a tube with this discharge length. The attainment of such an output will be dependent also on further optimization of the output mirrors.

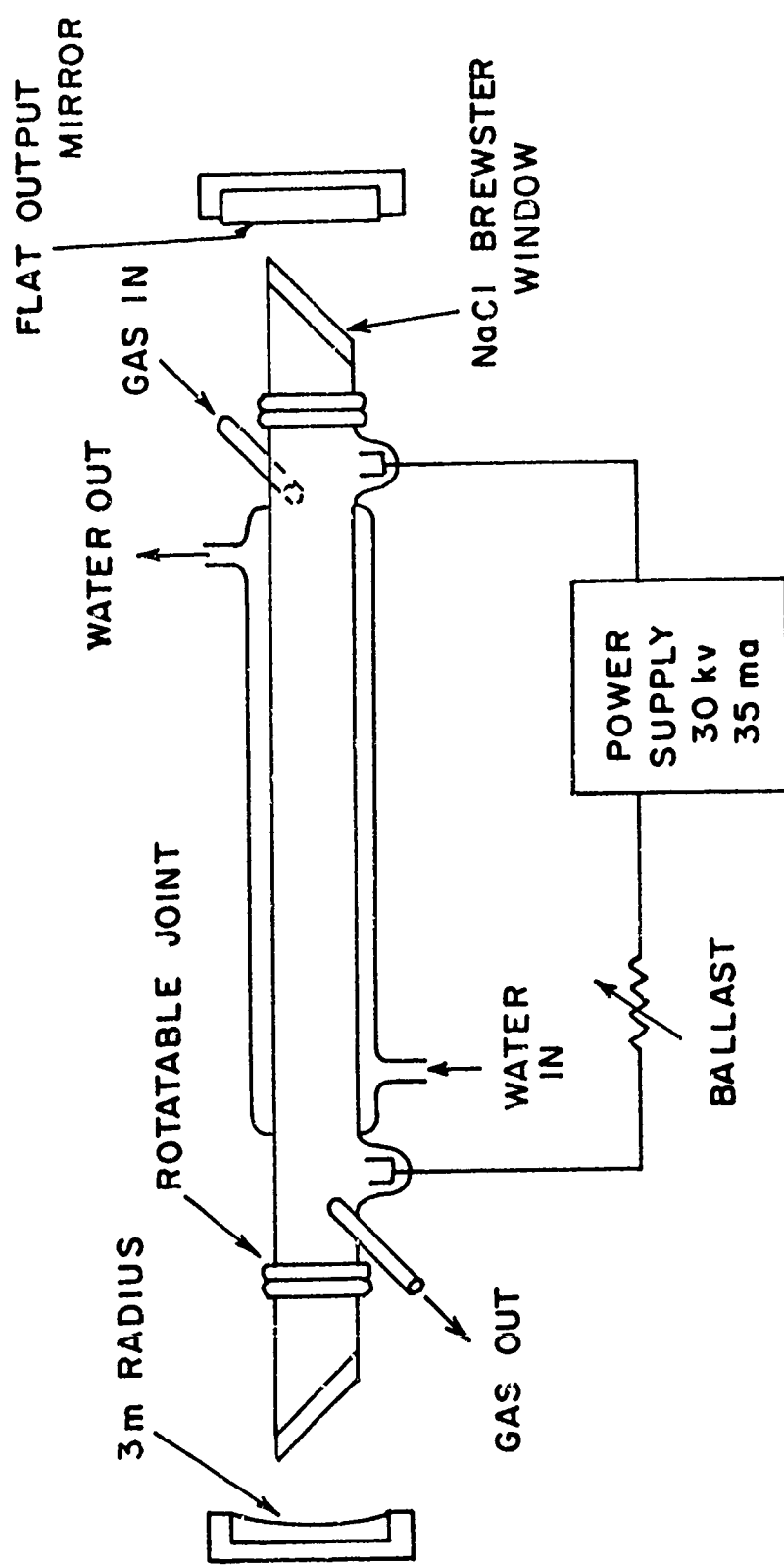


Figure II-1. Schematic of 1.25-meter Discharge Length CO₂ Laser.

B. Q-SWITCHING OF CO₂ LASER

Early in this reporting period we performed some experiments in Q-switching of the 50 cm discharge length CO₂ laser. The Q-switching was done by replacing the total reflecting mirror with a rotating prism mirror assembly. The prism was rotated using a dc motor with a maximum speed of 24,000 rpm. With the motor rotating at 20,000 rpm (330 Hz) the average power output dropped from 20 watts cw to .08 watt. The pulses were monitored with a mercury-cadmium-telluride detector cooled to 77°K and fed directly into a 1A1 Tektronix preamplifier. The apparent width of the pulses at the base was 1.8 μ sec. If this were the true width, the peak power in each pulse would only be 125 watts; however, we feel that it is possible that the width is due to the detector response in this case. Some more checking of the detector response will be done. However, we felt that even if there was some pulse broadening due to the detector response, that the enhancement of the output in the Q-switched mode was not sufficient to warrant further Q-switching of the small laser. We are now in the process of constructing a Q-switch consisting of a spinning double-concave gold-coated mirror which we will use to Q-switch our 125 cm CO₂ laser. We hope that by using the concave mirrors in the Q-switch (three meter radius of curvature) we will eliminate some of the jitter in the pulse size that was observed upon Q-switching the smaller laser with a rotating flat mirror. We feel that some of the instability in the pulse amplitudes was probably due to the vibration of the rotating mirror in the vertical plane which led to cavity misalignment.

C. SPECTROSCOPY OF LASER-PRODUCED PLASMA

The optical emission from a laser-produced plasma is being investigated in order to try to determine the characteristics of the plasma near the surface of the target being irradiated. The plasmas are produced by the irradiation of different solid targets with the focused beam from a carbon dioxide laser. It is hoped that the information obtained from spectroscopic data will complement that obtained from mass spectroscopic studies on the laser-produced

plasmas from metals. In the mass spectrometric studies, one of the difficulties encountered with interpretation was due to the fact that the properties of the particles emitted from the target surface were measured a long distance away from the region of interaction with the laser beam and it was difficult to deconvolute the information obtained. Thus, the spectroscopic information taken at the site of the optical interaction should eliminate the difficulty and answer some of the questions that are not yet clear.

The carbon dioxide laser cannot produce the high flux densities that can be obtained from Q-switched ruby lasers, and one might suspect that the interactions observed would differ considerably from those produced by Q-switched ruby lasers. However, if the mechanism of interaction of the laser beam with the expanding plasma in front of the target is inverse Bremsstrahlung, then the cross section for absorption at 10.6 microns (which is the wavelength output of the carbon dioxide laser) is over 3000 times larger than that at 7000 Å (corresponding to the output of the ruby laser). Therefore, the reduced flux density obtainable from a cw carbon dioxide laser is compensated for by the larger absorption cross section.

D. SPECTROSCOPIC MEASUREMENTS

We have previously reported ⁽⁷⁾ the photoelectric observation of the sodium D lines in the emission from the plasma produced in front of a glass target by radiation from a carbon dioxide laser. These lines were difficult to observe because of their low intensity as well as the presence of a very large amount of noise in the detector output. The low intensity could be attributed to the very slow evaporation rates produced by our carbon dioxide laser. We also experienced difficulty in obtaining the line spectrum because of the apparent diffusion of sodium out of the glass and the subsequent quenching of the D lines. The very large amount of noise observed on the photoelectric traces was probably due to strong turbulence in the plasma in front of the target.

Because of these difficulties we have changed out method of measurement from a photoelectric to a photographic spectrograph. The experimental setup being used is shown in Figure II-2. The change from a photoelectric to photographic spectrometer was made simultaneously with the start of operation of the larger carbon dioxide laser that produced a much more intense plasma in front of the glass target. The radiation from the carbon dioxide laser is focused onto the target with a five centimeter focal length Irtran 2 lens which is protected from the evaporant by a sodium chloride plate. With a laser output of 35 watts focused onto a spot approximately .01 centimeter in diameter, a bright plume of material about .5 centimeter long is observed being emitted from the target; the plasma is shown in Figure II-3. The light from the plume is collimated using a 9.5 cm focal length spherical lens made of borosilicate glass. The collimated light is then focused on the slit of a 1.5 meter grating Bausch and Lomb spectrograph using a 15 cm focal length cylindrical lens, also made of borosilicate glass. The fact that the lenses are made of glass means that any ultraviolet emission lines will be strongly attenuated.

The spectra are recorded on ten inch long strips of 35 millimeter film. We have been using Tri-X panchromatic film because of its high speed and fairly flat response over the spectral region of interest. This film, however, may not have the best characteristics for spectroscopic work and we may change to a different film in the future. Multiple spectra can be recorded on the same strip of film, using different exposure times, by the use of a sliding mask on the slit. A typical spectrum from a soda-lime glass is shown in Figure II-4. Some masking of the negative was done during printing to get the proper contrast; thus, relative intensities on the figure are not meaningful. The bottom trace shows the spectrum of a sodium spectral lamp used for calibration. All the other traces consist of the emission of the plasma taken with different exposure times. Most of the discrete lines have been identified and their origin and wavelength are shown in Table II-1. The assignment of atomic species was made using the known composition of the glass target given below:

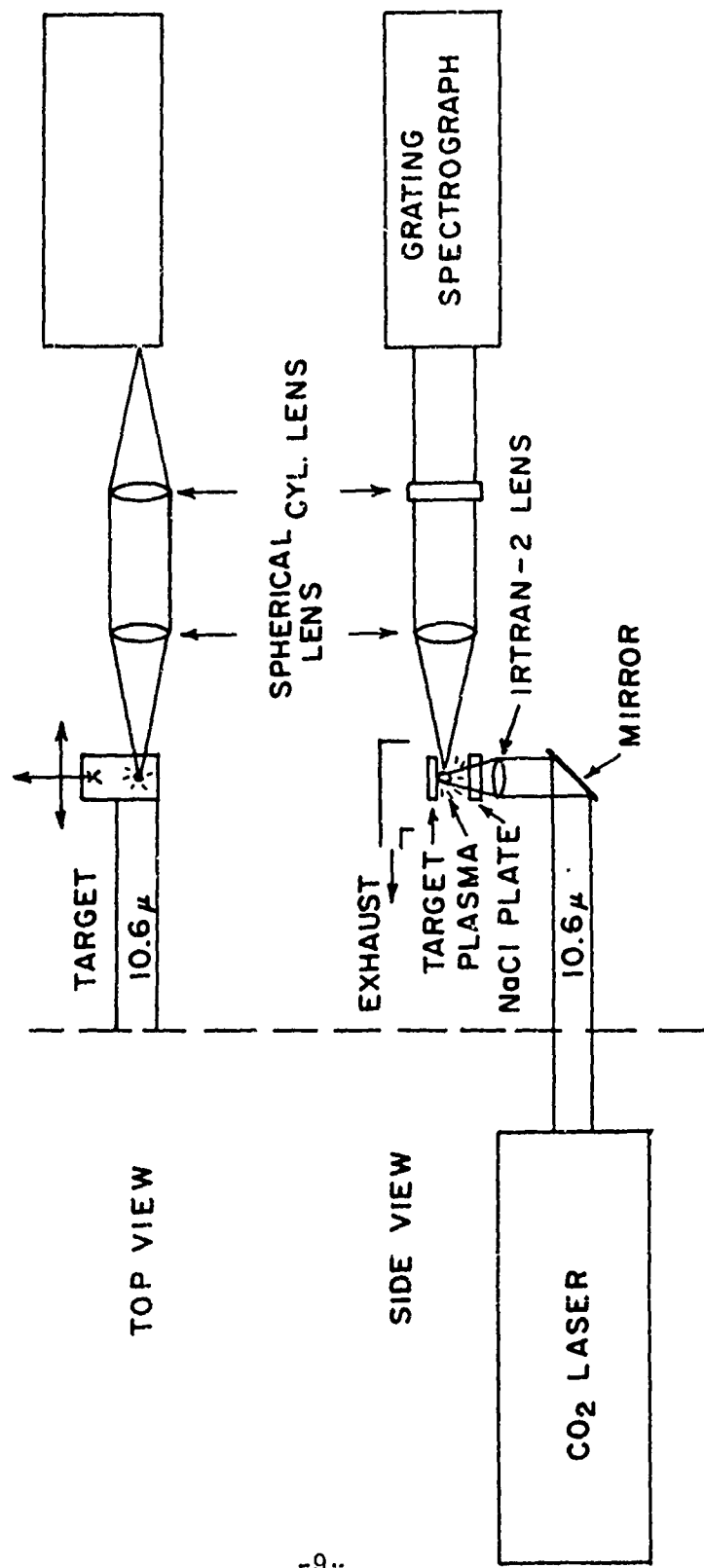


Figure II-2. Experimental Set-up for Photographic Recording of Spectrum of Laser-Produced Plasma.

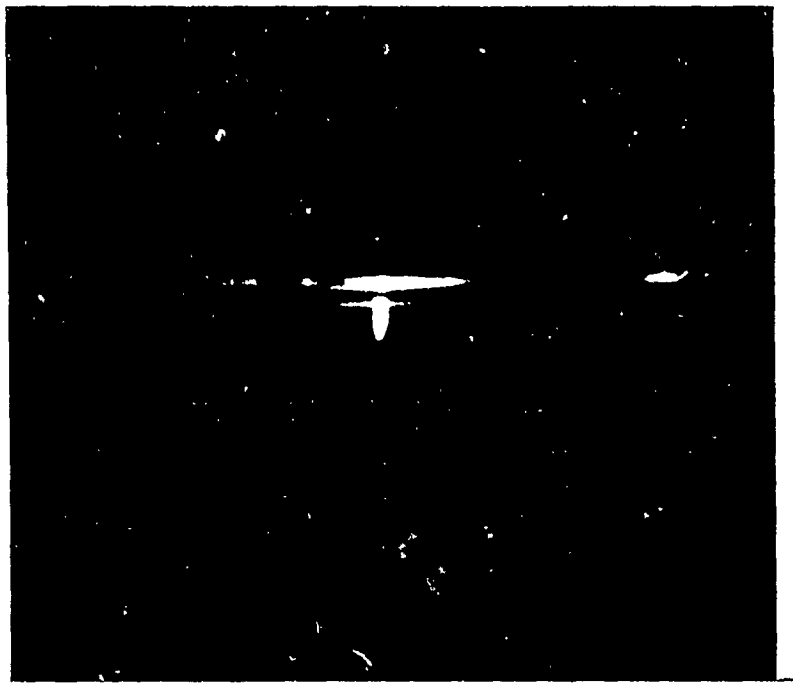


Figure II-3. Photograph of Plasma in Front of Glass Surface. Horizontal lines are the edges of the glass target. The length of the glowing plasma is ~ 0.5 cm.

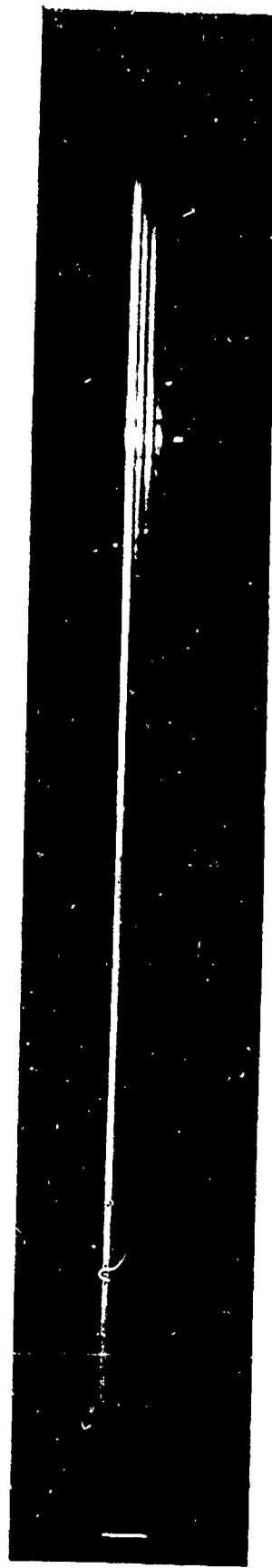


Figure II-4. Visible Spectrum of Plasma Produced by Laser Irradiation of Glass. Bottom trace is spectrum of sodium spectral lamp used for calibration. All other traces are spectra of laser-produced plasma obtained with different exposure times.

TiO_2	0.03%
SiO_2	72.5%
Fe_2O_3	0.15%
Al_2O_3	1.1%
CaO	8.7%
MgO	3.7%
Na_2O	13.3%
K_2O	0.1%
B_2O_3	0%
SO_3	0.3%
As_2O_3	0.1%

There may be short wavelength emission lines in the spectrum of the plasma that are not recorded in our experiment because of attenuation in the glass collimating optics. The glass has a cutoff at about 3300 \AA and therefore the wavelengths shorter than that will be very strongly attenuated. It can be seen that most of the lines have been identified and the majority of them are due to emission from sodium. The emission from the alkali metals, sodium and potassium, can be easily recognized by the doublet structure that characterizes single electron spectra. One of the most striking features of the spectrum is the reversal of the sodium D lines. These are by far the strongest lines in the spectrum and we felt at first that the reversal might be due to saturation of the film since the intensity of these lines was much greater than all the other ones. However, as shown in Figure II-4, we have reduced the exposure time of the film to the point where the region in the neighborhood of the D lines is far from film saturation and we still see this reversal.

The actual reversals of the D lines is not surprising since we have a plasma that is expanding in air and is cooling very rapidly. Therefore the outer layers of sodium atoms are much cooler than the hot interior and the resonance radiation will be strongly absorbed as it is emitted from the core and moves toward the spectrograph. That there is a very strong temperature difference between the emitting region and the absorbing region is evidenced by the fact that the emission line is much broader than the absorption line.

In fact, we hope to be able to use the difference in width between the emitted line and the absorption line as one method of inferring the temperature of the central region of the plasma.

One of the surprising features of the spectrum is that while there is a strong reversal of the D lines, the 3300 Å line, which we have tentatively assigned to be the unresolved resonance doublet of the sodium transition $4^2P \rightarrow 3^2S_{1/2}$, does not show any signs of reversal. This is a point that will be investigated further in the future using a quartz lens to reduce some of the attenuation produced by the glass lenses being used to focus the radiation on the spectrograph. This lack of reversal is also apparent in the emission from the 4044 Å doublet corresponding to the resonance transition of potassium $5^2P \rightarrow 4^2S_{1/2}$.

The spectrum obtained from glass serves as an example to illustrate the fact that we can use the cw carbon dioxide laser to produce plasmas that emit line radiation of at least the neutral species. We plan to use the relative intensities of these lines together with the known oscillator strengths for the transitions involved ⁽⁹⁾ to determine the temperature of the plasma in the region of interaction with the laser. We may also be able to use the reversal of some of the resonance lines to have another check on the temperature of the plasma.

In the experiments described in this section, we have used only glass as a target material because it is a convenient source of sodium ions which have strong spectral lines and it can be readily obtained. This does not mean that glass is the target material that we will use in the experiments on heating of the plasma, but simply that we will use it for initial practice. Our subsequent effort will concentrate on refining the method of production of the plasma and the detection method using the spectrograph and concentrating on a line emission from one atomic species as we vary the laser flux density and the pressure into which the plasma expands upon evaporation from the target.

We have investigated the emission from other target materials early in this reporting period when we had only a 20 watt CO₂ laser available. With the flux density available upon focusing that laser with a five centimeter focal length lens, we were not able to cause any considerable amount of evaporation from targets such as lithium niobate, sodium lithium niobate, calcium titanate, or barium titanate. More recently we have been able to evaporate samples of calcium titanate but the evaporation rate is much slower than that induced in glass due to the very high vaporization temperature of this material. We eventually plan to use targets with large amounts of alkaline-earth metals, for those have configurations suitable for our measurements in their neutral and singly ionized states.

TABLE II-1

Line Spectrum of Plasma Produced by Laser-Irradiation of Glass

Wavelength (nm)	Atomic Origin of Line	Transition	Reference
3305.2	Na	$4^2P \rightarrow 3^2S_{1/2}$	a
3356.7(?)			
3719.8	Fe		c
3736.9	Fe		c
3745.8			
3859.9			
4044.4	K	$5^2P_{3/2} \rightarrow 4^2S_{1/2}$	b
4047.4	K	$5^2P_{1/2} \rightarrow 4^2S_{1/2}$	b
4227.5	Ca		c
4498.8	Na		c
4666.3	Na		c
4670.0	Na		c
4750.0			
4753.0			
4980.6	Na	$5^2D \rightarrow 3^2P_{1/2}$	a
4984.3	Na	$5^2D \rightarrow 3^2P_{3/2}$	a
5151.0	Na		c
5155.5	Na		c
5685.4	Na	$4^2D \rightarrow 3^2P_{1/2}$	a
5690.6	Na	$4^2D \rightarrow 3^2P_{3/2}$	a
5890.0	Na	$3^2P_{3/2} \rightarrow 3^2S_{1/2}$	a
5895.9	Na	$3^2P_{1/2} \rightarrow 3^2S_{1/2}$	a
6156.8	Na	$5^2S_{1/2} \rightarrow 3^2P_{1/2}$	a
6163.5	Na	$5^2S_{1/2} \rightarrow 3^2P_{3/2}$	a
6713.4(?)			

- a) A. C. G. Mitchell and M. W. Zemansky, "Resonance Radiation and Excited Atoms," Cambridge University Press, New York, N. Y. (1961).
- b) C. E. Moore, "Atomic Energy Levels," NBS Circular 467, U. S. Government Printing Office, Washington, D. C. (1949).
- c) Handbook of Chemistry and Physics, 37th ed., Chemical Rubber Publishing Co., Cleveland, Ohio (1955).

III. WORK ON THE RUBY LASER AND HEMISPHERICAL INTERACTION CHAMBER

A. PICOSECOND PULSES

We have investigated the possibility of a picosecond duration substructure contained within the envelope of our Q-switched laser pulse. If such substructure exists, instantaneous powers much higher than the average value would be produced. Since this could affect the experimental results, it should be investigated and included in our analysis if necessary.

We used a technique similar to the two-photon fluorescence experiment described in the literature.⁽¹⁰⁾ The laser beam traverses a cell containing a benzene solution of the dye 9,10-diphenylanthracene and is reflected back on itself by a dielectric mirror at the end of the cell. The experimental arrangement is shown in Figure III-1. The pictures were taken in a dark room with the camera at f/4.7 using Polaroid type 47 packet film. The camera shutter was held open while the laser was triggered. The system allowed monitoring of the laser output on an oscilloscope. The dielectric mirror was aligned with an autocollimator. The blue fluorescence excited by two-photon absorption in the dye was photographed through a red rejecting filter and appears usually as a uniform streak along the path of the laser beam.

Occasionally the bright spots which have been interpreted as showing picosecond pulsing were observed along the track. The conditions of laser flux, film exposure, camera focusing, and so on, have varied widely. We feel that the appearance of the uniformly illuminated tracks is truly indicative of the fluorescence on most of the pulses for which this experiment was carried out, i. e., the bright spots indicative of enhanced two-photon fluorescence were not present. At the time the two-photon fluorescence experiment was carried out, the output of the phototube viewing the laser emission showed no ripple indicative of substructure in the 50 nanosecond duration laser pulse.

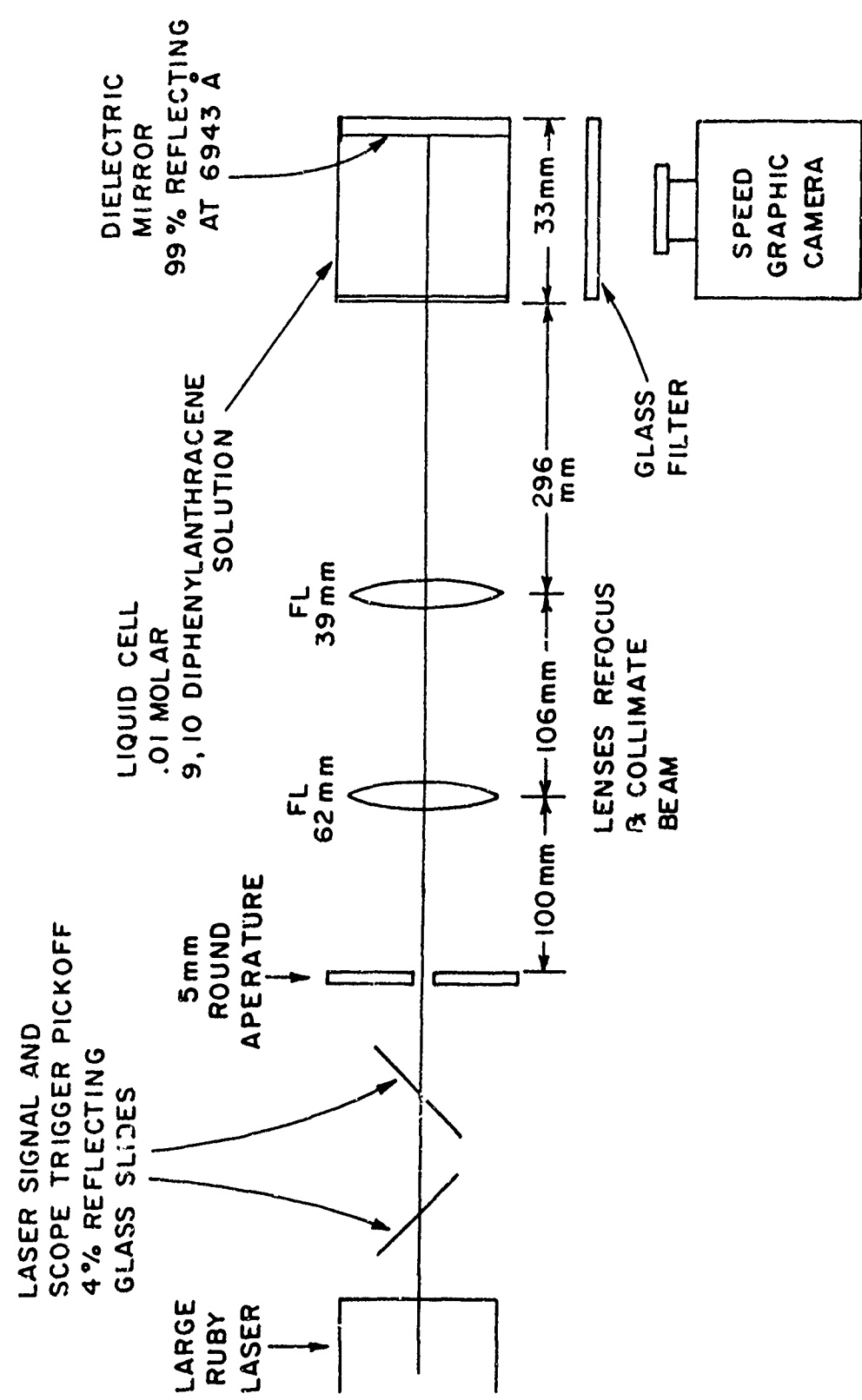


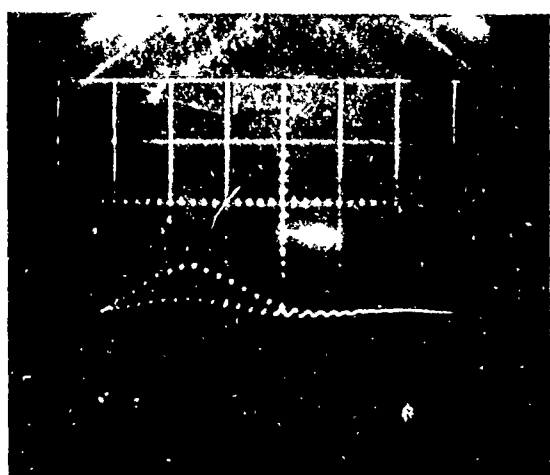
Figure III-1. Experimental Arrangement for Two-Photon Fluorescence Experiment.

On the few occasions on which bright spots were present, their dimensions and spacings were such as to indicate pulse durations of the order of 10 picoseconds and separations of the order of 200 picoseconds. With this setup we concluded that the operating conditions, as they existed at the time of this experiment, were such that picosecond duration pulses were occasionally present, but for the most part were absent. Conditions under which the picosecond pulses would be present were not well defined. Photographs showing the bright spots are not printed here because it is felt that they would not reproduce satisfactorily.

After the end of the two-photon fluorescence experiment, operating conditions apparently changed so that the oscilloscope presentation showed that nanosecond duration pulsations were present most of the time. The reasons for this change in the operation are not clear. Typical trains of pulses are shown in Figure III-2, which shows the output of a biplanar diode viewing the emission displayed on a 519 oscilloscope. The time scale is 20 nanoseconds per division. Pulses in this train can be quite regular. (See Figure III-2a.) We feel that the time constant of the detector system is fast enough that this represents the true behavior and that there is a background level with the time duration of 50 nanoseconds with the pulsations superimposed on top of it. It is possible that the peak amplitudes of the spikes in this train are so short that the detector cannot resolve them.

This pulse behavior is not reproducible. In some pulses the spiking is virtually absent, in others it may be present and damp out during the middle of the pulse (Figure III-2b), and at other times there is a clear double pulse structure, such as is shown in Figure III-2c. The period of these oscillations is about 4.5 nanoseconds, corresponding well to the round time for the 67 cm optical length cavity. This is strong evidence for a mode-locked nature for these oscillations.

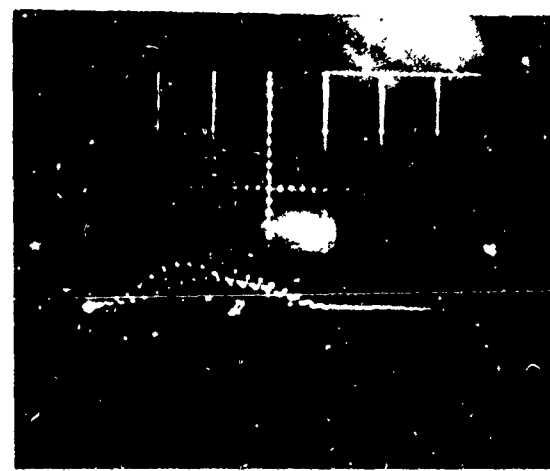
A double pulse structure with a spacing between the double pulses of $2d/c$ (where d is the distance from the saturable absorber to the nearer mirror) may originate because pulses arrive simultaneously at the absorber and have less absorption than pulses which arrive singly. ⁽¹¹⁾ The separation between



(a)



(b)



(c)

Figure III-2. Mode-locked Pulse Trains from Ruby Laser. Time increases from left to right at 20 ns/div.

pulses in the observed double pulse structure (see Figure III-2c) does not correspond obviously to the geometrical structure of our laser. The double pulse structure which is sometimes present is quite erratic and we do not have a firm explanation for it.

Picosecond substructure may well be present within the mode-locked nanosecond structure shown in Figure III-2. Such structure can arise from the presence of various parallel surfaces within the laser cavity.⁽¹²⁾ Therefore, since operating conditions have shifted since our earlier negative result on detection of picosecond pulses, we plan to search for them again under the present operating regime.

We should note that in a careful analysis of the two-photon fluorescence experiment, it is necessary to measure the contrast in the photographs carefully. A number of free-running modes with random phases can interfere to give enhanced fluorescence, but the contrast ratio will be less than for the mode-locked case.

B. RUBY LASER MEASUREMENTS

Experimental work has included investigation of the emission from a tungsten target at higher laser flux densities than had been employed previously in the hemispherical interaction chamber. The laser flux density at the target surface was of the order of 1000 megawatts/cm², about one order of magnitude higher than the flux density at which previous measurements had been carried out. The characteristics of the emission from the detectors around the periphery of the hemisphere were qualitatively similar to what was observed previously.^(6, 7) The shapes of the pulses are approximately the same as before; however, the amplitudes are approximately one order of magnitude greater than what was produced with the lower flux densities. Figure III-3 shows typical examples of the pulses from collector No. 5 at an angle of 15° from the normal to the target surface. The time scale is five microseconds per division and time increases from left to right. The vertical amplitude is 0.1 volts per division. Data taken under similar circumstances but with a

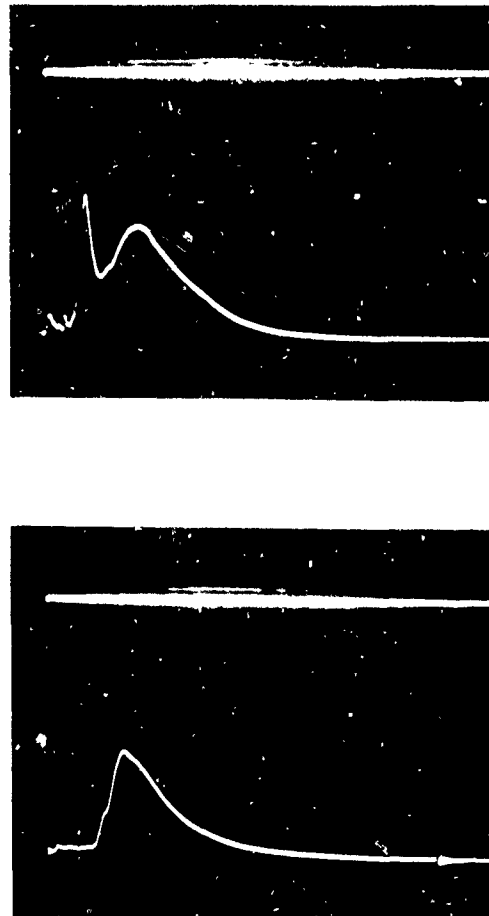


Figure III-3. Typical disc collector outputs for laser flux density $\approx 10^9$ w/cm².
Time increases from left to right at 5 microseconds/div.
Vertical amplitude is 0.1 volts/div.

laser flux density of the order of 10^8 watts/cm² incident on the target surface gave an amplitude about one order of magnitude smaller.

When the target is removed from the hemisphere, is it apparent that some vaporization of the base material has been produced. Therefore, the earlier conclusion that the particle emission consists mainly of materials present on the surface, such as CO, CO₂, and sodium and potassium ions, may not be applicable to the bulk of the particles making up these signals. The fraction of the signal in Figure III-3 which is produced by tungsten atoms is not known. In order to investigate this point, futher measurements should be made using the time-of-flight spectrometer at higher laser flux densities and under conditions where some of the base material is removed from the surface. In these measurements on the hemisphere, there are no measurements that use mass discrimination that would allow us to identify the material definitely.

Measurements have also been made using the bipolar collector.⁽⁷⁾ The total ion collection from the bipolar collector is about one order of magnitude higher than at the lower laser flux densities. The signal can reach a level of 80 volts across a 500 picofarad capicitor, or a total charge collection of the order of several times 10^{11} electron charges. A typical example is shown in Figure III-4. Multiplying by a factor of 10^3 for the solid angle (including the anisotropy factor) would imply a total ion production of the order of several times 10^{14} per laser pulse at the position of the target. This result will be used later in an analysis of the possible heating of the blowoff material. The results indicate that the phenomena occurring at the higher laser flux densities are qualitatively similar to what occurs at the lower flux densities, but that more material is removed and more ions are produced.

In an effort to investigate the role of the surface in affecting the observed results and in influencing the directed expansion of the particles,⁽¹³⁾ we shall carry out an experiment in which the target is a very thin foil, which will easily be punctured during the laser shot. Each laser shot will then, of course, be incident on a different point of the target. If the conjectures on the role of reflection from the surface in producing the directed expansion are

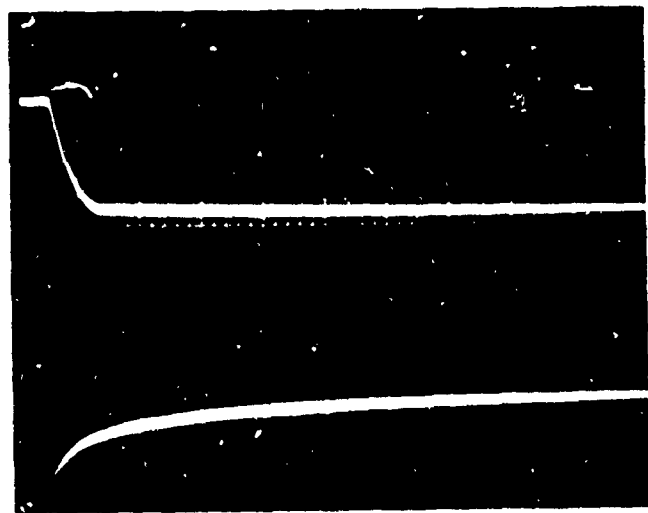


Figure III-4. Typical signal from bipolar collector for laser flux density $\approx 10^9$ w/cm². Time increases from left to right at 5 microseconds/div. Upper trace shows electron collection at 200 volts/div. Lower trace shows ion collection at 50 volts/div.

correct, allowing the surface to be evaporated during each laser pulse should make a difference in the angular distribution. This experiment will also allow us to compare the total numbers of atoms removed from the foil to the numbers registered at the collectors.

IV. ANALYSIS

A. CALCULATED PLASMA HEATING

Previous measurements (2) on the time-of-flight spectrometer indicated initial ion densities of the order of 10^{13} to 10^{14} per cubic centimeter near the surface of the target. This was derived from measurements in which the number of ions per pulse was estimated to be of the order of 10^9 . These measurements were carried out at laser flux densities of the order of 10^8 watts/cm². Measurements on the bipolar collector, which we feel to be a more reliable indication of total ion production, indicate particle densities of perhaps 10^{19} cm⁻³ (7) at the same laser flux density. Recent measurements (Section III) have extended the measurements to approximately 10^9 watts/cm² and the charge collection at the position of the bipolar collector is correspondingly higher. These results have revived interest in calculating heating of a plasma by inverse Bremsstrahlung.

Previous calculations had indicated that densities in excess of 10^{19} particles per cubic centimeter would be required to produce the observed heating. (6) At that time we did not believe that such densities were actually produced. However, with the measurements on the bipolar collector indicating much higher total charge production, we infer that the plasma densities near the target may be higher than we believed and that faster heating rates are possible.

The computer program to calculate the heating, which had been run earlier (6), was adapted to be suitable for larger ion densities. This required modification of a number of equations in the program. At the higher densities the equations would be carried outside the limit of their validity. In particular, this is true for calculation of the factor $\log..$ which represents the collective effects in the plasma. The equation used previously was (14)

$$\log.. = 1.5 \left(\frac{k^3 T^3}{\pi N_e} \right)^{1/2} Z^2 e^3$$

where N_e is the electron density, Z the charge of the ion species under consideration, and T the temperature. This equation is no longer applicable for very high density plasmas at relatively low temperatures. There is no good information in the literature concerning an appropriate form for the collective effects in this case. Therefore, this factor was arbitrarily set equal to unity when the plasma density exceeded the range of validity of the equation above, that is, collective effects were neglected. This procedure is conservative in that, if anything, heating effects will be underestimated by this procedure.

The calculation of the shift in ionization potential ΔE also had to be modified. For low electron densities ΔE is a small correction; however, for larger densities where ΔE becomes greater than about 0.2 times the ionization potential, the original form of the equation was not suitable. ⁽¹⁵⁾ It is suggested ⁽¹⁶⁾ that above a certain critical electron density

$$N_c^{CR} = \frac{1}{2\pi} \left(\frac{kT}{e^2} \right)^3$$

the form for the ionization potential change be given by

$$\Delta E = 6.45 e^2 N_e^{1/3} - \frac{kT}{2} \log \left(\frac{N_e}{N_e^{CR}} \right) - 1.5 kT$$

At the critical value of electron density, this formula gives only a slightly different result from the old formula, but for $N_e > N_e^{CR}$, the values are different. The net effect of this change is that smaller shifts in the ionization energy are calculated as the electron density becomes very high. This means that in the Saha equations:

$$\frac{N^Z}{N^{Z-1}} = \frac{2Z^Z(T)}{Z^{Z-1}(T)N_e} \left(\frac{mkT}{2\pi n^2} \right)^{3/2} \exp \left[- \frac{E^{Z-1} - \Delta E^{Z-1}}{kT} \right]$$

where N^Z , Z^Z , and E^Z are respectively the ion density, partition function, and ionization energy for ionization stage z ⁽¹⁵⁾ which is the basic equation used in the calculation, the argument of the exponential will be larger negatively than would have been calculated by the old formula, and therefore the ratios N^{Z+1}/N^Z will be smaller than calculated under the old formula.

The results of the program indicate very rapid heating for a laser flux density of 10^8 watts/cm² and initial particle densities in a sodium plasma of 10^{19} , 3×10^{19} , and 10^{20} per cm³. See Figure IV-1. From the bipolar collector results, we believe these numbers to be a reasonable order of magnitude for the original particle density. The assumption that all of the material is sodium is rather arbitrary in this case, since it is possible that a large amount of the vaporized material may no longer be easily ionizable alkali ions. Therefore, this calculation should be repeated with the appropriate parameters for a material such as tungsten or carbon.

The basic results indicate that the heating can be very rapid. Heating to a temperature of the order of 10 eV occurs in a short time compared to the laser pulse length. Ionization to highly ionized stages occurs in this process. The routine is of limited validity after the temperature reaches approximately 20 eV because of the high values of the ionization calculated.

Another point is worth mentioning: For low particle densities and temperatures of the order of 5000°K, sodium is almost entirely singly ionized. The ratio N^+ / N^0 is large. This ratio is inversely proportional to the electron density (from the Saha equation). At total particle densities below about 10^{18} cm⁻³, N^+ / N^0 remains large enough that the material is essentially fully ionized. However, as the total particle density reaches 10^{19} , N^+ / N^0 becomes of the order of magnitude of unity and the material is not fully ionized. For an initial particle density of 10^{20} per cubic centimeter at 7000°K, the material is only 15% ionized. This has the effect that the heating rate (for the particle densities used in Figure IV-1) in the first few nanoseconds is relatively insensitive to the total particle density because an increase in total particle density tends to lower N^+ / N^0 . This effect is visible near the left edge of Figure IV-1. For higher values of the initial particle density, the initial heating causes a more rapid increase in electron density, because the ionization is a very strong function of temperature. Therefore, after the first few nanoseconds, the heating rate becomes approximately linearly dependent on the initial particle density. At 12,000°K, for example, singly ionized material becomes dominant for an initial particle density of 10^{20} cm⁻³ and

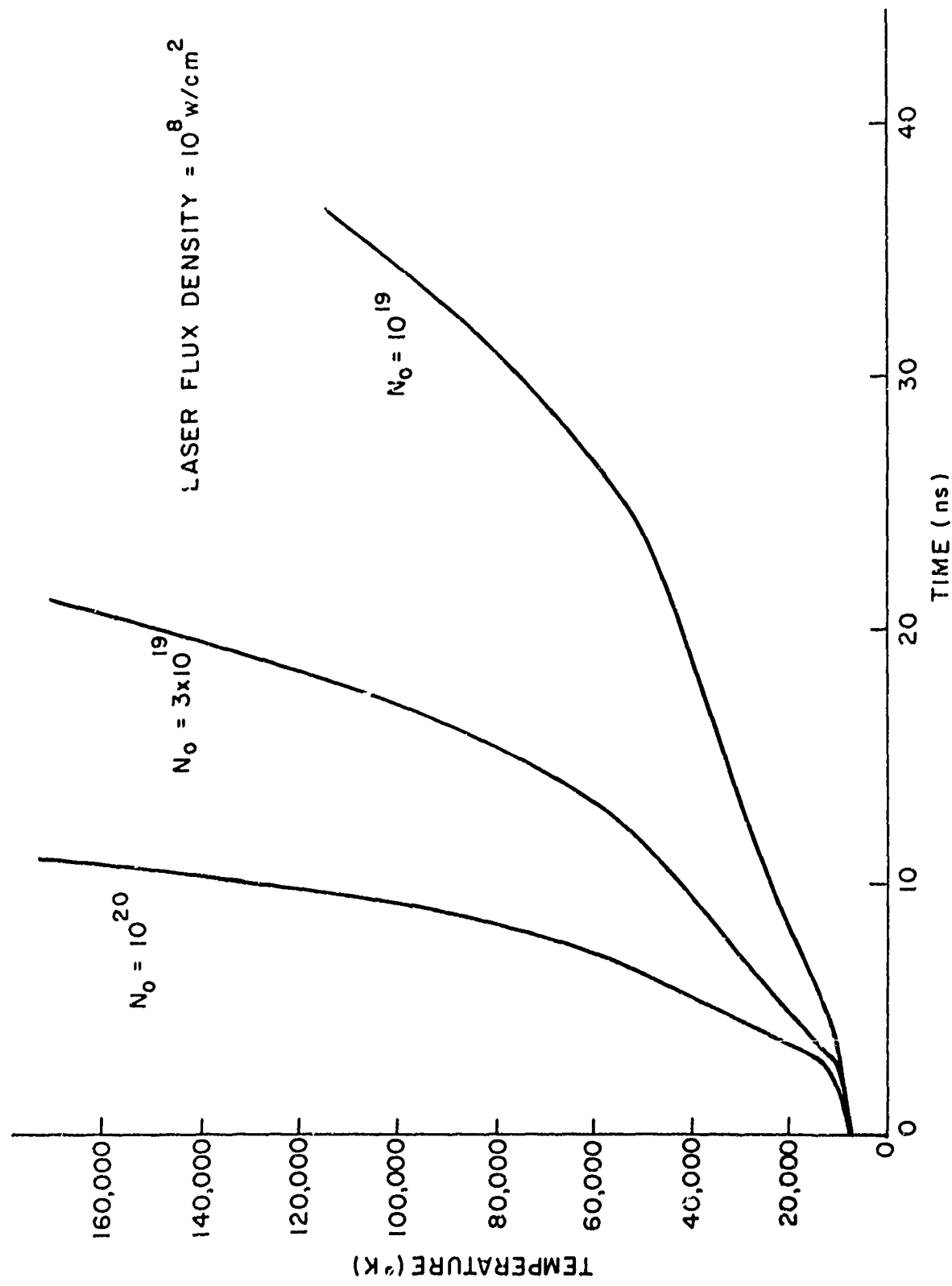


Figure IV-1. Calculated Heating of Sodium Plasma as a Function of Time for Various Initial Total Particle Densities N_0 .

the electron density will be an order of magnitude greater than for the case of an initial particle density of 10^{19} cm^{-3} .

Heating proceeds to approximately $40,000^\circ\text{K}$ with the singly ionized material being dominant. At that point doubly ionized material becomes important and the heating rate takes another upward increase. The routine is limited by the fact that only nine ionization states of sodium are considered. For temperatures of the order of 20 eV, sodium would become more than eight times ionized so that this routine is not valid at very high temperatures.

A summary of results of this computer calculation is that heating to temperatures of the order of 10 eV in times comparable to the laser pulse length are reasonable for flux densities of the order of 10^8 watts/cm^2 (which is representative of our experimental conditions), and for initial particle densities of the order of 10^{19} cm^{-3} or greater. Below particle densities of 10^{19} cm^{-3} , little heating is expected. For particle densities $\geq 10^{19} \text{ cm}^{-3}$, the heating rate is almost independent of the initial particle density for the first few nanoseconds. When the temperature becomes greater than approximately $12,000^\circ\text{K}$, the plasma is essentially fully singly ionized and the heating rate is approximately proportional to the initial particle density. At $40,000^\circ\text{K}$ second ionization becomes important and the heating rate increases again. As the temperature reaches 10 to 20 eV, the material becomes very highly ionized.

B. EXPANSION OF HEATED PLASMA

These calculations did not include any provision for expansion of the material. This is not a realistic assumption. In order to include expansion of the heated material, a modification was made in the main program so that the total particle density would decrease according to the equations for adiabatic expansion. In previous report ^(5, 6) we calculated that the pulse shapes obtained at a collector some distance from the target were well approximated by the adiabatic free expansion of a pulse of gas heated to a few tens of eV near the surface of the target. As the gas expands, we would expect that the heating rate would drop because of the form of the equation for the absorption coefficient. Therefore, the routine was modified to include the expansion

according to this equation. Results are presented in Figure IV-2 for the case of a laser flux density of 10^8 watts/cm² and initial particle densities ranging from 3×10^{19} to 3×10^{20} particles per cubic centimeter. Early in the laser pulse we again see that the heating rates are roughly comparable for the various initial total particle densities. This reflects the same factor that was described earlier, namely, the decrease in the amount of ionization as the total particle density increases. Again there is a rapid increase in heating rate as the temperature rises to 12,000°K and a second jump near 40,000 to 50,000°K, reflecting the regions where the material becomes essentially fully singly ionized and approximately fully doubly ionized. The heating rates are somewhat slower than in the case where no expansion was considered. Even allowing for expansion, considerable heating still can be obtained in reasonable times for particle densities greater than approximately 3×10^{19} per cubic centimeter. Therefore, the inclusion of expansion in the basic equations does not appreciably affect the main conclusions but means that a slightly higher initial particle density would be required.

C. COMPARISON TO EXPERIMENT

Now let us compare these results to what we would expect from experiment. From old data taken on the bipolar collector at laser flux densities of the order of 10^8 watts/cm² we find⁽⁷⁾ that a voltage of approximately 3.5 volts was produced in a 500 picofarad capacitor in an integrating circuit. This corresponds to a total charge collection of 1.75×10^9 coulombs or approximately 10^{10} electron charges. Including a factor of 10^3 for the relative solid angle (including the anisotropy factor) this leads to a total charge production of the order of 10^{13} per laser pulse. This does not show up on the disc collectors because we have hypothesized⁽⁷⁾ that the material travels as a neutral plasma and the main effect on a disc collector is observed as secondary electron emission which is produced by both positive and negative particles.

The postulated total production of 10^{13} to 10^{14} from an area of the order of 0.01 cm^2 and the assumption of thermal velocities leads to densities of several times 10^{19} cm^{-3} for total densities near the target. Later results

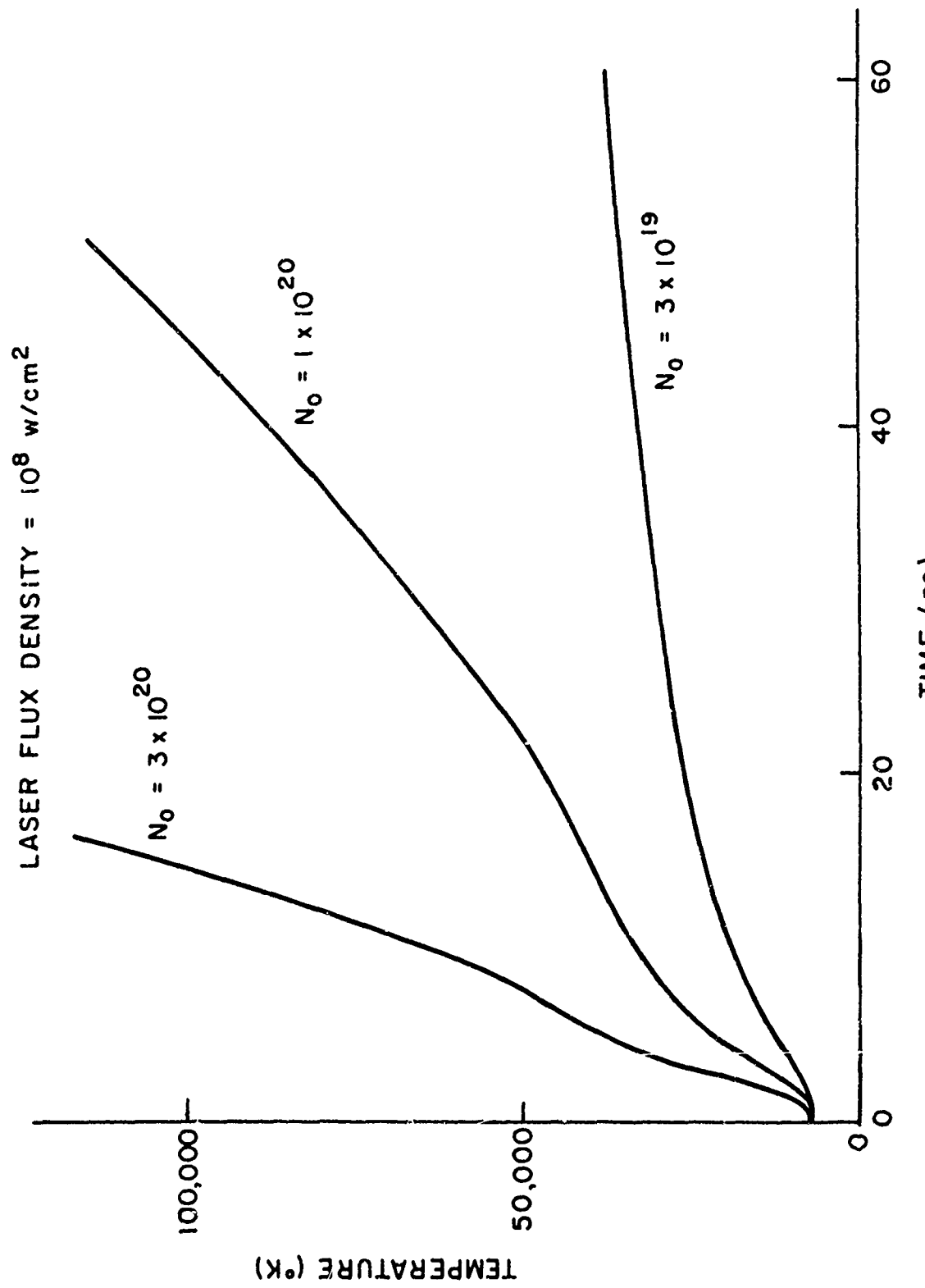


Figure IV-2. Calculated Heating of Sodium Plasma as a Function of Time, With Inclusion of an Expansion of the Plasma, for Various Initial Total Particle Densities N_0 .

(see Section III) taken at 10^9 watts/cm² indicate still higher total charge production so that the values would be greater than 10^{20} cm⁻³ at times early in the laser pulse. Thus it appears that our experimental measurements indicate ion densities large enough to be compatible with rapid heating by this mechanism.

These results may be also compared with what would be expected from evaporation. In reference (17) the vaporization rate of carbon at a temperature of the order of 8000°C was taken as 3920 grams/cm²/sec. For a thermal velocity of 3.4×10^5 cm/sec, this would imply a density of 6×10^{20} cm⁻³. Also, the density inferred from analysis of the expansion of the blowoff material, and of the impulse transferred to the target in a steady state model, indicated a density near the surface of a tungsten target of the order of 10^{19} cm⁻³ for a laser flux density of 10^8 w/cm². (13) Thus the ion densities used to obtain the results of Figure IV-1 seem reasonable if the target material can be raised to high temperatures and be evaporated at an appreciable rate by the laser pulse.

These results also seem reasonable in light of the earlier calculations on pulse shapes arising from an adiabatic free expansion of laser-heated material. If the blowoff material is heated to a temperature of the order of a few tens of eV in a time of the order of a few tens of nanoseconds and then expands, the pulse shapes calculated (5, 6) are very similar to the pulse shapes actually observed in our apparatus. This present result indicates for the first time that we can actually expect to achieve sufficient heating under our experimental conditions.

In Section III-B we noted that the pulse shapes produced in the hemispherical interaction chamber are qualitatively similar for laser flux densities varying over an order of magnitude. Let us consider why this is so. As the calculations described above show, for a plausible initial particle density, and for laser flux densities of the order of 10^8 w/cm², heating rates can be large enough that temperatures of the order of a few tens of electron volts can be reached within the time of the laser pulse. According to the earlier analysis on the pulse shapes produced by adiabatic free expansion, (5, 6) this is all

that is necessary to produce our experimental pulse shapes. Thus, over a fairly wide range of conditions, rapid heating can occur. At higher laser flux densities the heating rate will increase, but also the material will expand more rapidly. Thus, the density will drop faster and cut off the heating earlier. The observed pulse shapes will not be a strong function of the laser flux density and the phenomena observed at different laser powers are qualitatively similar.

D. EFFECT OF SURFACE ON ISOTROPY OF BLOWOFF MATERIAL

Now let us consider the role the surface plays in producing the observed results and, in particular, its influence in producing a directed component to the expansion. One calculation⁽¹³⁾ has indicated that the surface introduces an anisotropy in which particles reflected from a lattice of fixed particle sites tend to be emitted at angles closer to the surface normal than the angle at which they were incident. In fact, it has been shown that under some circumstances it might be possible to obtain a reasonable approximation to a $\cos\theta$ distribution, where θ is the angle from the normal. This is in reasonable agreement with our experimental results.^(6, 7)

A complete comparison of the experimental results to a theory would require considerably more work. The calculations in Reference⁽¹³⁾ considered only two different angles. In order to specify the distribution completely, the calculation should be carried out for a number of angles of incidence and the distribution functions for the angles of reflection calculated. Then these results should be integrated over a Maxwellian velocity distribution to provide a complete specification of the angular distribution of the reflected material. It is anticipated that this would require a great deal of work. The basic result simply indicates that the material can be emitted in directions closer to the normal than the angle at which the particles struck the surface originally, and this would tend to produce a directed motion of the material away from the surface.

There have been experimental studies which have investigated the angular distributions of ions reflected from various metallic surfaces. Most of this

work is fairly old. (18, 19) The experimental results indicate that the situation is complicated and that the angular distributions of the reflected ions depend on the nature of the reflecting surface, the temperature of the reflecting surface, the incident ion energy, the energy transfer in the collision and on other parameters. The published results do not give a complete and comprehensive view of this phenomenon and in some cases appear to be contradictory. The results of some authors indicate that many of the secondary reflected ions are ejected as if they were reflected at the specular angle, that is, the angular distribution of the reflected particles has a maximum near the angle for specular reflection.

Other authors' results indicate complicated angular distribution functions for the reflected ions. In many cases it appears as if the reflected ions tend to be shifted toward more grazing angles than the incident beam, that is, the maxima in the distribution functions lie at larger angles from the normal than the incident beam. This result is the opposite of what the analysis in Reference (13) would indicate. For other ranges of ion energy, there appears to be a shift toward the normal in the maximum of the distribution function. The position of the maximum in the angular distribution of the reflected ions undergoes a definite shift toward the normal for ion energies of the order of 100 eV. In some instances there is strong evidence for a component of the reflected ions to be directly along the normal. In one experiment (19) 500 eV lithium ions were incident on a nickel surface at an angle of 51.5° from the normal to the surface. There was a very strong maximum in the reflected ions along the normal. These results indicate that at least for some ranges of experimental parameters, the analysis in Reference (13) is in accord with experimental data.

In a recent paper (20) the particle flux and speed distributions for molecular argon and nitrogen beams of lower energy (0.065 to 0.24 eV) scattered from polycrystalline stainless steel and nickel surfaces showed angular distributions of the reflected particles that were definitely shifted toward the normal. Thus, we conclude that while the experimental picture is not completely clear, there is at least some evidence that indicates that the directed energy of the laser-produced material can be explained by reflections from the surface and by a

shift in the angular distribution toward the normal in the manner discussed in Reference (13).

Moreover, the theoretical results do tend to indicate an angular distribution that is in reasonable agreement with the angular distribution measured in the laser surface interaction.⁽⁶⁾ This seems to indicate that the surface does play a role in producing the directed energies of the particles.

Another point worth considering is the origin of the high energy neutral molecules. If the surface does play a role in reflecting the particles, this may help explain the production of copious numbers of high energy neutral particles observed. Hagstrum's results⁽²¹⁾ indicate that the cross section for reflection of ions as metastable neutral molecules is large. The currents of metastable neutral molecules are considerably larger than the reflected ion currents. Reflection with neutralization may lead to an increase in kinetic energy equal to

$$\delta E = E^{z-1} - E_m - \Phi - E_c$$

where E^{z-1} is the ionization energy of state (z-1), E_m is the excitation energy of the metastable particle, Φ is the work function of the surface, and E_c is the energy transferred to the lattice in the collision (typically a small fraction of the original kinetic energy). Thus, the rather large ionization energies of the highly ionized states can effectively be converted into potential energies in a metastable atom. For highly ionized species this energy can be quite large. If the metastable atom subsequently undergoes a collision, this energy may be released as kinetic energy. The presence of hydrogen in the neutral molecule emission⁽³⁾ may be enhanced because the reflections favor transfer to atoms of low atomic number. This hypothesis about energy transfer has a bearing on the effect that the surface may play in producing the observed results. If heating occurs to temperatures of the order of tens of electron volts, such a process could be important in causing the directed nature of the expansion and in causing recombination and production of high energy neutral molecules.

There is another point to be considered about the adiabatic free expansion. If material is reflected from the surface and the expansion becomes essentially one-dimensional, there is an increase effectively of a factor of three in the total energy available, because originally the energy was partitioned equally among the three perpendicular directions. This would help explain the directed nature of the expansion.

V. CONCLUSIONS

The following specific conclusions can be derived from the work described in the previous sections.

1. Carbon dioxide lasers can produce plasmas which show strong spectral emission. The advantages of long wavelength and high repetition rate available from the CO₂ laser suggest that this will be a valuable tool in studying the laser-surface interaction. Direct temperature measurements on the laser-produced blowoff material appear to be possible.
2. A negative result has been obtained on a two-photon fluorescence experiment which was designed to investigate the possible presence of picosecond duration substructure in the laser pulse. It appears that the occurrence of picosecond pulsations is not a completely general feature of Q-switched laser operation.
3. Measurements in the hemispherical interaction chamber have extended the measurements into a new regime of laser flux density, up to 10⁹ watts/cm². The results obtained at this flux density are qualitatively similar to what was observed previously. The amplitudes of the pulses are greater. The results have been analyzed to indicate that the total ion production is of the order of several times 10¹⁴ ions per pulse and that particle densities in excess of 10¹⁹ per cubic centimeter can be produced near the target surface.
4. The results of a computer program in which the heating of a sodium plasma is calculated indicate that temperatures of the order of a few tens of electron volts can be obtained in a time comparable to the laser pulse duration for particle densities which appear to be reasonable. These results are compatible with our earlier observations of the fact that the particle pulse shapes are in agreement with a model in which the material is heated to a few tens of electron volts and then undergoes an adiabatic free expansion.

5. The experimental angular distribution measurements are qualitatively similar to results obtained from an analysis of the effect of reflections at the surface. This analysis explains the directed nature of the expansion by reflections which shift the maximum of the angular distribution toward the normal.

A number of avenues for further investigation in the next report period are indicated. We shall obtain higher peak powers by Q-switching the carbon dioxide laser. We intend to estimate the temperature of the plasma produced by the CO₂ laser from the spectroscopic measurements, and also to carry out an experiment in which the repetitively pulsed CO₂ laser radiation interacts with the plasma and heats it. We shall also investigate new target materials, particularly those containing alkaline earth elements.

Using the ruby laser, we intend to carry out measurements in the hemispherical interaction chamber in which the target will be a thin foil punctured by a single laser shot. A measurement of the hole diameter will give an accurate indication of the total number of atoms released in the laser-surface interaction. This may be compared to the data obtained from the different collectors. In addition, if the angular distributions are dependent on reflection of particles from the surface, this experiment should indicate a somewhat different angular distribution for the emitted material. We hope, also, to carry out measurements on the time-of-flight spectrometer at higher laser flux densities than were previously employed. We will thus determine the composition of the blowoff material, and in particular the fraction that consists of the target material, at a laser flux density of 10⁹ watts/cm².

We also feel that it would be worthwhile to extend the computer program described in Section IV. Of particular interest would be analysis of data representative of carbon and tungsten targets. This could be done by substituting the appropriate parameters for the various excited levels of these atoms as input data to the computer program. As part of a more comprehensive analysis of the phenomena occurring in the laser-surface interaction, the

entire range of phenomena covered by the computer program could be extended. The absorption of laser radiation as a function of depth within the expanding material, continued heating of the surface and ejection of new material into the plasma at the surface, the impulse transferred to the surface, expansion of the material, and the temporal pulse shape of the laser, could all be incorporated into such a model.

Finally, we shall also employ the two-photon fluorescence technique to search for possible picosecond duration substructure under the new operating conditions of the laser.

REFERENCES

- (1) "Mechanisms of Laser-Surface Interactions," by J. F. Ready, E. Bernal G., L. P. Levine, Final Report to Ballistic Research Laboratories on Contract DA-11-022-AMC-1749(A), March 1965. (AD-467, 867)
- (2) IBID, Semi-Annual Report on Contract DA-11-022-AMC-1749(A), Mod. 2, November 1965. (AD-477, 231)
- (3) IBID, Final Report on Contract DA-11-022-AMC-1749(A), Mod. 2, May 1966. (AD-636, 680)
- (4) IBID, by J. F. Ready and E. Bernal G., Semi-Annual Report on Contract DA-18-001-AMC-1040(X), December 1966. (AD-645, 473)
- (5) IBID, by J. F. Ready, E. Bernal G., and L. T. Shepherd, Final Report on Contract DA-18-001-AMC-1040(X), May 1967. (AD-654, 524)
- (6) IBID, Semi-Annual Report on Contract DA-18-001-AMC-1040(X), Mod. No. 1, November 1967. (AD-666, 245)
- (7) IBID, Final Report on Contract DA-18-001-AMC-1040(X), Mod. No. 1, May 1968. (AD-672, 093)
- (8) "High Power Laser Research," D. R. Whitehouse, Final Report on Contract DA-01-021-AMC-12427(Z), May 1967. (AD-653, 031)
- (9) "Experimental Transition Probabilities for Spectral Lines of Seventy Elements" by C. H. Corliss and W. R. Bozman, NBS Monograph 53, U.S. Government Printing Office, Washington, D.C. (1962).
- (10) M. A. Duguay, S. L. Shapiro, and P. M. Rentzepis, Phys. Rev. Lett. 19, 1014 (1967).
- (11) J. A. Fleck, Jr., J. Appl. Phys. 39, 3318 (1968).
- (12) M. A. Duguay, International Quantum Electronics Conference, May 1968. Paper 4O-4.
- (13) F. J. Allen and O. R. Lyman, Studies of the Effects Produced by Laser Beam Bombardment of Surfaces, BRL Report #1373, August 1967. (The report is confidential; these references refer to unclassified sections of the report.)
- (14) L. Spitzer, Physics of Fully Ionized Gases, p. 72, Interscience (1956).
- (15) H. R. Griem, Plasma Spectroscopy, McGraw-Hill (1964), Ch. VI.

(16) E. P. Duclos and A. B. Campbell, Z. fur Naturforschung 16A, 711 (1961).

(17) F. J. Allen, A Determination of the Surface Temperature of a Target Heated by an Intense Laser Beam, BRL Report #1394, February (1968).

(18) R. W. Gurney, Phys. Rev. 32, 467 (1928); G. E. Read, Phys. Rev. 31, 629 (1928); M. A. Eremeev and M. V. Zubchaninov, J. Exp. Theor. Phys. 12, 358 (1942); A. Longacre, Phys. Rev. 46, 407 (1934).

(19) R. B. Sawyer, Phys. Rev. 35, 124, 1090 (1930).

(20) S. S. Fischer, O. F. Hagen, and R. J. Wilmoth, J. Chem. Phys. 49, 1562 (1968).

(21) H. D. Hagstrum, Phys. Rev. 123, 758 (1961).

Unclassified

Security Classification

DOCUMENT CONTROL DATA - R & D

(Security classification of title, body of abstract and fixating information must be entered when the overall report is classified)

1. ORIGINATING ACTIVITY (Corporate author)

Honeywell Incorporated
Corporate Research Center
Hopkins, Minnesota 55343

2a. REPORT SECURITY CLASSIFICATION

Unclassified

2b. GROUP

3. REPORT TITLE

MECHANISMS OF LASER-SURFACE INTERACTIONS

4. DESCRIPTIVE NOTES (Type of report and inclusive dates)

Semi-Annual Report

5. AUTHOR(S) (First name, middle initial, last name)

J. F. Ready and E. Bernal G.

6. REPORT DATE

November 1968

7a. TOTAL NO. OF PAGES

46

7b. NO. OF REFS

21

8a. CONTRACT OR GRANT NO.

DA-18-001-AMC-1040(X) Modification No. 2

9a. ORIGINATOR'S REPORT NUMBER(S)

b. PROJECT NO.

c.

9b. OTHER REPORT NO(S) (Any other numbers that may be assigned this report)

d.

10. DISTRIBUTION STATEMENT

This document has been approved for public release and sale; its distribution is unlimited.

11. SUPPLEMENTARY NOTES

12. SPONSORING MILITARY ACTIVITY

U.S. Army Aberdeen Research and Development
Center
Ballistic Research Laboratories
Aberdeen Proving Ground, Maryland 21005

13. ABSTRACT

This report describes investigations of the mechanisms by which high power laser radiation interacts with absorbing surfaces. Construction of a carbon dioxide laser used in this work is described, along with preliminary spectroscopic observations of the emission produced when this laser radiation interacts with a glass target. Measurements of ion emission produced by a ruby laser beam with flux densities of the order of 1000 megawatts per square centimeter incident on a tungsten target have been analyzed. From the results it is estimated that particle densities of the order of 10^{20} per cubic centimeter are produced near the target surface. A computer program using these particle densities has been employed to calculate the expected amount of heating produced by absorption of the incident laser radiation in a sodium plasma of this density. The results indicate that rapid heating to temperatures of the order of tens of eV is possible within the time of the laser pulse duration.

DD FORM 1 NOV 68

1473

REPLACES DD FORM 1472, 1 JAN 64, WHICH IS
OBsolete FOR ARMY USE.

Unclassified

Security Classification

Unclassified

Security Classification

14. KEY WORDS	LINK A		LINK B		LINK C	
	ROLE	WT	ROLE	WT	ROLE	WT
Laser Effects Plasmas Ion Emission High Power Spectroscopy						

Unclassified

Security Classification